CORROSION OF SILVER ELECTRICAL CONTACTS: THE SUBSTRATE INFLUENCE

Constantine T. Dervos and Panayota Vassiliou

National Technical Univ., Athens, Electrical and Computer Eng. Dept, Chemical Eng. Dept, 9, Iroon Polytechniou Str.Zografou 15773, Athens, Greece.

ABSTRACT

Silver and silver based alloy (90% Ag- 10% CdO) contacts welded on different substrate materials have been exposed in hostile SO_2 environments in simulated laboratory conditions. The corrosion byproducts on the surface have been monitored by SEM and EDS spectroscopy. Their electrical characterization was based upon dc overheat tests, current switching cycle tests and interfacial energy storage during ac current excitation. The experimental results demonstrate that the heat dissipation rates strongly depend on the substrate material selection as well as, the exposure environments. These parameters strongly affect the nominal current values.
The dynamic contact resistance during make-break electrical contact operations depends upon the conductivity of the new surface layers formed as a result of chemical equilibrium established by the reaction between the environment and the primary surface material, the substrate, and the welding layers. Corrosion byproducts are formed over the contact joint and are transported to the silver surface of the electrical contact by creep. The resulting byproducts, may be either loosely attached or water-soluble. Corrosion products originate from the welding zone, the substrate material, and the underplating layer by diffusing through the pores of the plating; they aggregate on the surface and affect the heat dissipation rate and consequently the electrical performance of the component.

I. INTRODUCTION

Silver alloys, as well as the pure metal, have been proposed or applied for electrical contact applications and extensive laboratory and field studies of such systems have been carried out [1,2]. Several researchers measured the silver contact resistance, R_c, as a function of exposure time for components subjected to field locations[3-6]. Satisfactory contact performance is maintained as long as R_c remains below 10 mΩ [7]. In some locations R_c may increase over the course of a few years by five or six orders of magnitude [8,9]. Contact resistance has also been measured following laboratory exposure to mixed corrosive gases [10] where the rapid increase in R_c for contacts exposed to Cl_2 or H_2S has been demonstrated. Abbott [11] investigated several Ag/Au and Ag/Pd alloys in laboratory environments with H_2S. The resultant thin films were very tenacious and had high contact resistance. On the basis of chemical and contact resistance studies of silver alloys with 50% Au or 60% Pd Antler [8] reached essentially the same conclusions. Currently, the mixed flowing gas (MFG) tests are adopted for component characterization in adverse environments [12,13], but the relation between field and laboratory exposure yet remains to be determined.

SO_2 tarnishes silver but the metal is relatively insensitive to SO_2 as compared to H_2S. The reaction of silver with SO_2 to form sulfide and oxide is not thermodynamically favorable. A reduction path for SO_2 with sulfide as a possible end product was proposed and involves dithionite, $S_2O_4^{2-}$, as an intermediate specie[14]. In this work, the approach of "accelerating degradation SO_2 environment" is used to study surface induced effects and degradation mechanisms on silver based electrical contacts welded on different substrate materials. It is true that *static* single-gas laboratory tests, including those of SO_2, have largely been discredited as being unrealistic of the reactions occurring in the real word. However, due to the increased severity of the influencing parameters, the rate of the degree of deterioration will increase, so that it can be measured during a short time interval. The basic idea is very simple: to artificially increase the concentration of the gaseous reactants to boost degradation rates without change of the mechanism of the chemical reaction thus producing faster deterioration. The applied test parameters could be met in practice under extreme field conditions, i.e. industrial accidents[15] (worst case analysis) or under dew formation on the metal surface at installations near complexes with high SO_2 emission rates. The pollutant concentrates on the surface forming sulfate nests. Therefore, even small

initial concentrations of SO_2 may turn out to become highly aggressive after such a cumulative process.

The scope of this work is to point out the significance of the substrate material selection, as far as, the long-term operation of the electrical component is concerned. The substrate material may control the overall heat dissipation rate during component operation, thus affecting the entire electrical performance. In addition, the substrate material can induce corrosion byproduct formation due to electrochemical reactions initiating degradation during the operation of the component in an adverse environment.

II. EXPERIMENTAL

The typical geometry of the examined contact joints is given in Figure 1. The electrical contacts had a planar geometry of 2.3 mm x 2.3 mm, consisting of high purity silver, or silver metal oxide (90% Ag, 10% CdO). These were welded on top of a brass (70% Cu 30% Zn) or copper substrate, by a three layer tape. The top welding layer was cadmium oxide (percentage 90% Ag and 10% CdO). The middle layer was pure Cu and the bottom layer was pure Ni which was employed primarily to add interfacial resistance, so that the tape could be safely welded to the substrate. The tape layers were hot bonded in a rolling mill in an inert atmosphere, thus producing a metallurgical bond. The rolling procedure could be extended to attain the desired thickness of the welding structure.

Some of the produced samples were also plated, either by silver flash process to create a high purity silver overlayer of 30 μm to 50 μm, or gold plated at a thickness of 25 μm. The gold plated samples had a 50 μm thick nickel underlayer. Plating was the last operation in the overall fabrication sequence. This resulted to a pure Ag or Au layer formation over the entire electrical contact region, the tape welding layers (which during rolling expand sideways around the contact edge) and finally, over the surface of the suspending wafer.

The following types of contact families were tested under accelerating degradation conditions:

- Ag on top of brass substrate
- Ag on top of copper substrate / Ag plated
- Ag/CdO on top of brass substrate

- Ag/CdO on top of brass substrate / Ag plated
- Ag/CdO on top of brass substrate / Au plated.

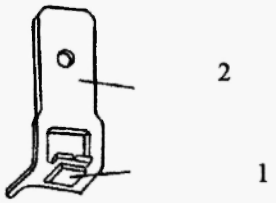

Fig. 1: Contact geometry. (1) silver based electrical contact with a planar surface 2mm x 2mm, (2) substrate. The contact is welded on the substrate by hot-bonded tape layers.

The above contact families were exposed to room temperature synthetic air mixtures incorporating 20% SO_2 and equilibrium humidity. The exposure duration was 24 hours. The specimens were removed, washed with distilled water to remove the soluble corrosion products, and their weight change was monitored. Reference samples were graphitized to become conductive to the electron beam and were examined by Scanning Electron Microscopy (SEM) and Energy Dispersive Spectroscopy (EDS) to obtain the percentage of the elements on the surface volume of the metal.

The samples were also subjected to electrical characterization tests prior and after the exposure to the hostile environment. The characterization consisted of:

(α) Temperature overheat tests (according to IEC 0660) to demonstrate the temperature rise across stationary contact joints as a function of time under dc and ac current excitation. The stimulating current waveforms were provided by a stabilized power supply capable of producing 20 A dc. Proportional temperature monitoring via a "T-type" thermocouple wire, attached at the vicinity of the contact joint, was preferred for comparison purposes. The operating air temperature was for all cases 18°C and the ambient relative humidity 55%.

(β) Contact resistance monitoring during mechanical duty cycles under dc current excitation. The mechanical apparatus used for the simultaneous application of electrical and mechanical load is presented in Figure 2. When the contacts closed, the applied axial contact force could vary between 0 and

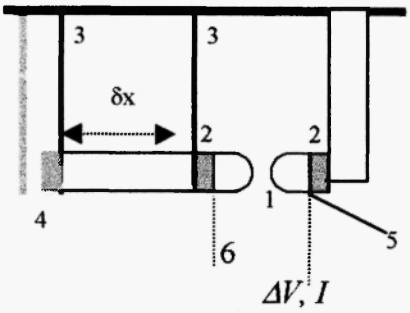

Fig. 2: Layout of the mechanical apparatus: 1) Electrical contact joints. 2) Electrical insulators. 3) Phosphor-bronze springs allowing linear displacement $\delta x \approx 3mm$. 4) Computer controlled magnetic circuit stimulating δx linear motion. 5) Location for temperature monitoring and transducer position for axial contact force measurement. 6) Flexible current leads. Interfacial voltage, ΔV, and current, I, profiles could also be synchronously recorded.

5N and this was monitored by a piezoelectric transducer, interfaced to a 20MSPS data logging system. A computer controlled apparatus was employed to operate hammer-action duty cycles, i.e. perform axial low amplitude contact displacements, by controlling the current values in a solenoid actuator which activated a closed-loop magnetic circuit. Each duty cycle lasted 6 seconds among which the contact was closed for a 3-second period. Contact transitions between states CLOSED and OPENED consisted of approximately 18 discrete low amplitude linear displacements, thus simulating contact bounce conditions, or contact blow-open effects. Relatively high current densities (ampacities of 17 A dc via contact areas of the order of 0.04 mm^2, optically determined) were employed in order to establish accelerated degradation modes of operation. The applied mechanical vibrations induced short arcs -as shown in Figure 3- possibly leading to phase transitions on metallic surfaces, or decomposition of the crept corrosion products. As a result, the examined contacts were simultaneously subjected to mechanical and electrical fatigue. Both of the above dissociation mechanisms are expected to affect the overall contact resistance. During the make-break operations the resistance variation across the contact joints was also recorded. Heat radiation from the stationary contact joint was monitored by a computer controlled IR thermometer

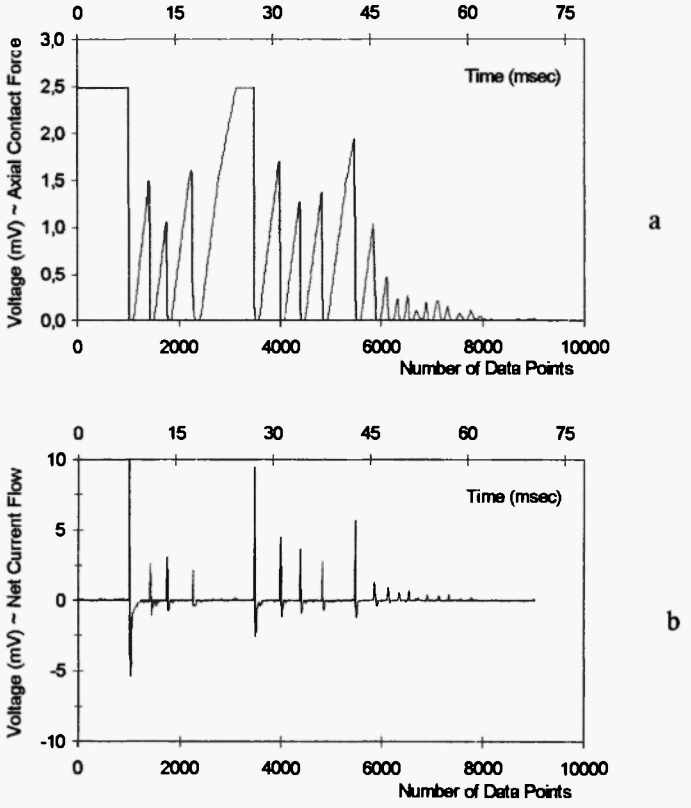

Fig. 3: **(a)** Typical axial contact force variations applied during the contact break transient state. The interfacial mechanical contact is broken several times (of the order of 20) for this specific case. **(b)** Transient over-currents recorded in the external circuit as a result of multiple contact make-break transitions. After completing the overall test cycle, the interface had sustained approx. 20,000 hammer-action finite amplitude displacements.

operating at 8-14 μm with a sampling period of 15 seconds. The measuring target was identified by a crossed beam pinpoint laser system. The emissivity value of the measuring targets was set at 0.2 for all cases.

(γ) Visual observations of interfacial energy storage during ac current excitation. Figure 4 provides the required experimental set-up. Closed contacts were energized by a stabilized sinusoidal current profile and

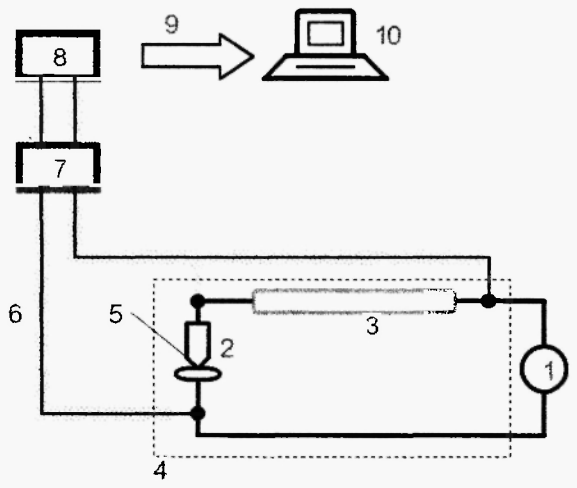

Fig. 4: Simplified schematic diagram of the overall experimental setup: **1)** 50 Hz sinusoidal current supply with maximum value 200 A rms even under short-circuiting operating conditions. **2)** Contact under test. **3)** OFHC ohmic loads varying between 10μΩ and 5mΩ, used for current monitoring. **4)** Environmental control chamber. **5)** Temperature transducer. **6)** Coaxial cable. **7)** Amplifier. **8)** I(t) and V(t) monitoring device: Synchronous data logger 12 bit 20MSPS . **9)** Data bus. **10)** PC

interfacial voltage V(t) and flowing current I(t) waveforms were digitally recorded and processed to provide the corresponding I-V curve (by time elimination).

For contacts operating under high current densities the resulting I-V curves tend to produce closed (clockwise) loops in a single period of the stimulating current profile-as predicted by the mathematical bifurcation theory [16,17]. The corresponding area of each loop determines the electrical power stored at the interface[18]. Precise knowledge of the period required to obtain each closed loop provides for the interfacial energy, E, evaluation. This can be attained – as shown in Figure 5 – by the sum of successive trapezoids according to the equation:

$$E = \tfrac{1}{2}(V_{n+1} - V_n).(I_{n+1} + I_n) \, . \, T \qquad (1)$$

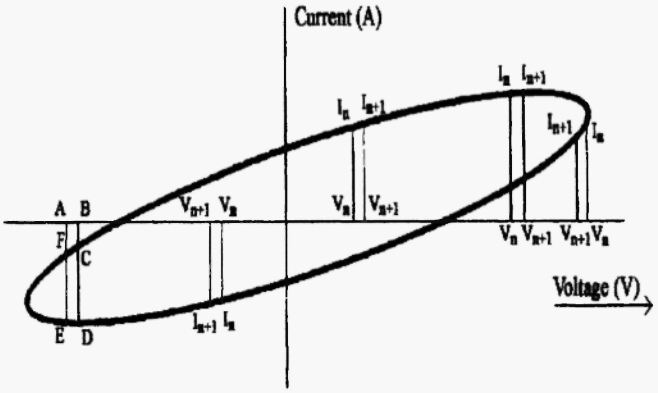

Fig. 5: Typical current- voltage loop shape, used for the determination of the electrical energy according to the Eq. 1. Various V_n and V_{n+1} as well as I_n and I_{n+1} positions have been introduced in this figure in order to demonstrate for every quarter of the axis that the areas of some of the trapezoids will be added while others will be subtracted. For example, in a clock-wise loop formation, the loop area determined by the letters FCDE will be evaluated by the proposed equation as the difference between ABDE and ABCF partial areas.

where V_n represents the n^{th} voltage value in volts, I_n represents the corresponding n^{th} current value in amperes, (synchronous result pair) and T, is the period required to produce a single closed loop, i.e. T=20 ms. The applied methodology, as well as, the advantages offered by such electrical tests have been reported elsewhere[19,20].

III. RESULTS AND DISCUSSION

A. Electrical Characterization

A1. Temperature overheat tests for stationary contacts – Figures 6a,b provide the typical normalized temperature increase vs. time of current flow, for the case of silver contacts welded on top of brass and copper substrates respectively. In the same figures, the effect of SO_2 exposure is also demonstrated. According to these results the non-corroded samples exhibit

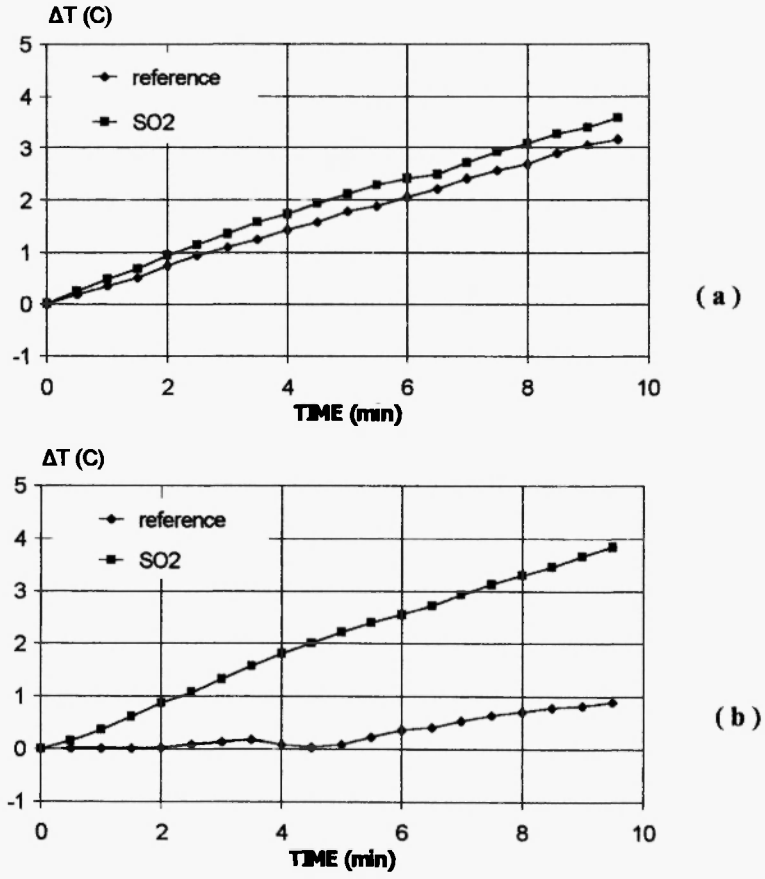

Fig. 6: Normalized temperature increase for stationary silver contacts excited by 20 A dc. Reference contacts are compared to contacts exposed to SO_2 environment.
(a) The substrate material is brass.
(b) The substrate material is copper/silver plated.

the lowest temperature gradients. In addition, the substrate material may significantly affect the overall heat dissipation rate and therefore determine the nominal current of the component. This is evident by comparing the temperature gradients among reference samples of Figures 6a and b (i.e. notice enhanced temperature increase on reference components with the brass substrates).

Finally, it should be noted that the silver contacts welded on top of the

brass substrates are protected from corrosion during SO_2 exposure compared to identical contacts on copper substrates (plated or not). At the same time the brass substrate appears to be heavily attacked, (formation of insulating copper-zinc sulfate salts overlayers). The corrosion formations have to be mechanically removed (by filing) to enable for electrical connection -over the clamping regions- during test procedures. Corrosion effects can be attributed to galvanic cell formation between the silver contact and the brass substrate, which effectively protects the silver end of the cell and increases the corrosion effects on the less noble material which is brass, thus leaving the silver electrical contact unaffected. As a result, there is scarcely any difference between the electrical performance of reference Ag/Brass samples and the ones exposed to SO_2 environment.

A2. Contact resistance under current switching cycles – Silver contact resistance was monitored in the process of switch iterations. The contacts were energized by 17 A dc. The open circuit voltage was 15V. As shown in Figure 7a, there is scarcely any difference between the contact resistance values of reference samples and of identical samples exposed to the SO_2 environment. The typical contact resistance of silver contacts welded on top of copper substrates is shown in Figure 7b. Here, the contact resistance of reference joints was significantly lower, due to incorporation of substrate-materials with higher thermal and electrical conductance. However, for this material selection, SO_2 exposure increased the overall contact resistance by 50% typical. For this material combination, there is no need to clean mechanically the surface of the substrate to attain proper electrical conductance, after SO_2 exposure.

The temperature generation rate of the joint, during the current cycling switching tests, was found to depend upon the substrate plating, as well as, the exposure to the SO_2 environment and to the induced damage. This is clearly demonstrated between Figures 8a,b.

According to the temperature data recorded by the infrared (8-14μm) energy data acquisition technique, Figure 8, the unexposed reference samples show between them very small temperature differences during the test procedure. The samples with the best electrical response appear to be the gold plated ones even after running 20,000 discrete current switching cycles. However, after being exposed to SO_2, the gold plated samples exhibit the highest heat generation rate and consequently the worst electrical response. Silver plated samples provide fairly stable behavior. The non-plated substrate

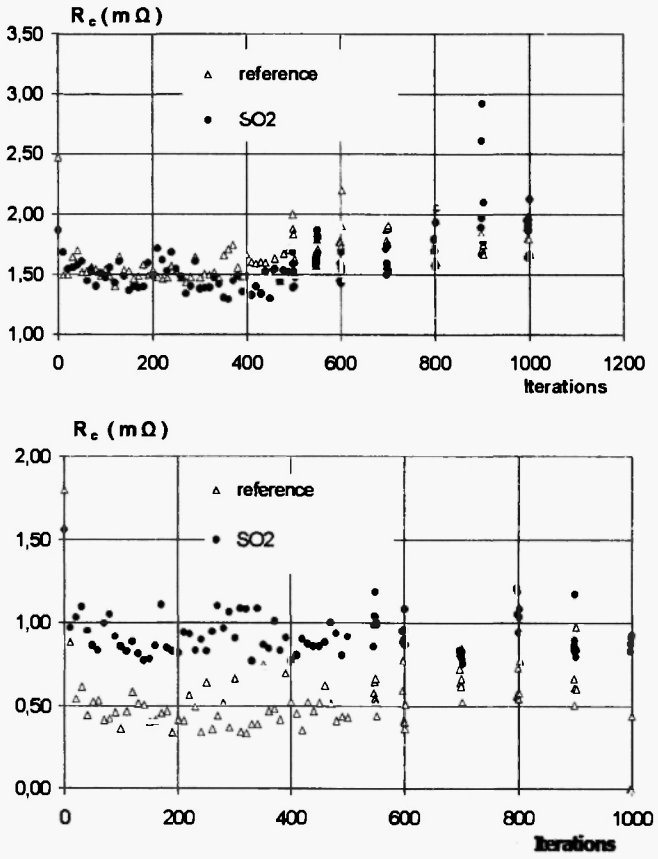

Fig. 7: Contact resistance for the reference contacts and the contacts exposed to SO_2 environment as a function of switch iterations. The test short circuit current was 20 A dc and the open circuit voltage was 15 V.**(a)** Contact material: silver welded on top of brass substrate. The substrate had to be cleaned (filed) at the clamping edge, to remove the insulating copper-zinc sulfate film, thus allowing for current conduction. **(b)** Contact material: silver, welded on top of copper substrate, and then, silver plated contact joint resistance, R_c, for the examined material selection was found to be 1.5 mΩ. This resistance was increased by 20% max. at the end of the switching cycle test (probably due to surface erosion).

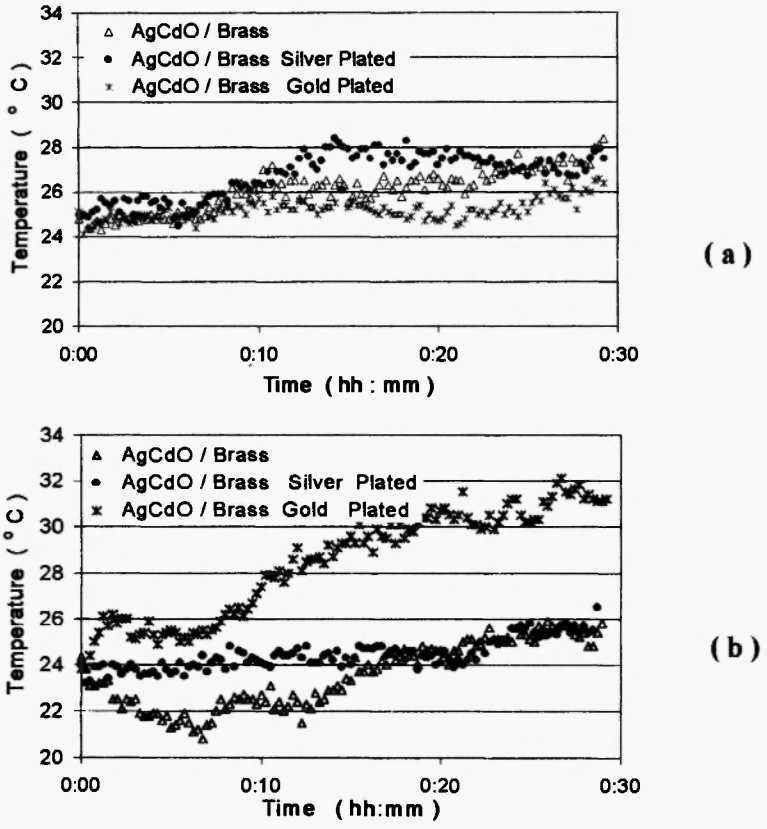

Fig. 8: Average stationary joint (anode) temperature as a function of time elapsing during current switching cycle tests. Iteration period = 6 s, I_{sc} = 17A dc, and V_{oc}=15V dc.(**a**) Reference samples. (**b**) Samples exposed to SO_2.

samples during their initial stages of operation showed negative temperature response (i.e. temperature reduction with increasing operation time) which can be possibly attributed to the insulating overlayer surrounding the contact material.

A3. Energy storage across stationary contacts during ac current operation – The electrical energy stored across the contacting joints during ac operation is visualized in Figures 9(a) and 9(b) for the case of silver contacts welded on brass substrates and silver contacts welded on copper substrates

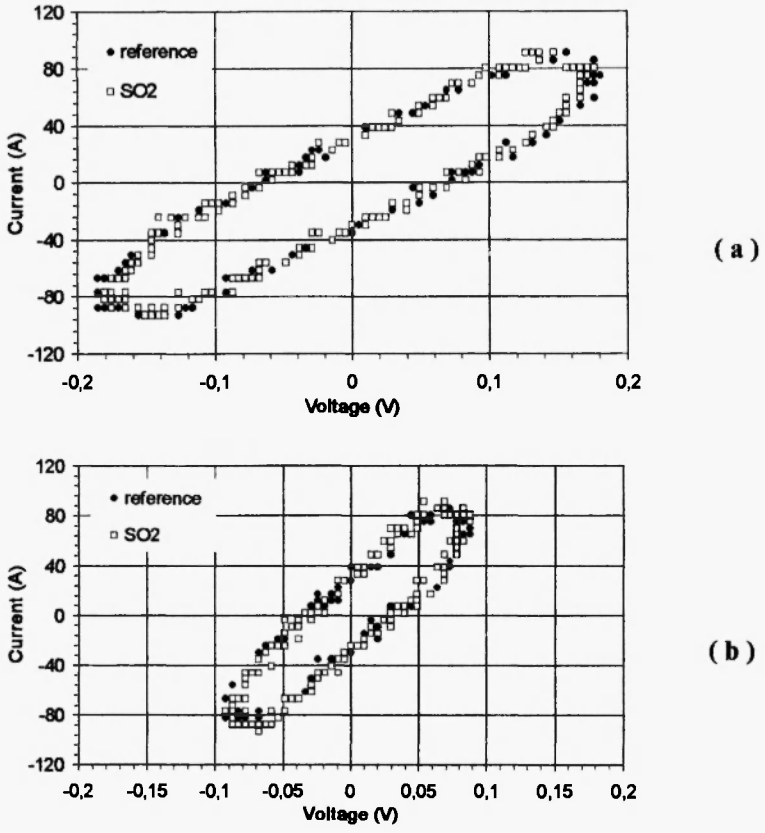

Fig. 9: Visual observation of the electrical response of different contact joints stimulated by 60 A rms 50 Hz current profiles.**(a)** Ag on brass, **(b)** Ag on copper/silver plated substrate. The time required for loop production is 20 ms. The results clearly demonstrate the substrate influence on the electrical response, as well as, the induced variations -if any- by component exposure to the SO_2 environment.

and then silver plated. For comparison purposes, the response of the same components is also exploited after their exposure to SO_2 aggressive environments. The obtained current-voltage loops are accomplished within 20 ms interval. The related power data averaged over 25 successive cycles have been evaluated and are summarized in Table 1. According to the presented results, silver plated copper substrates indeed tend to relieve the stored power across the electrical contact joints.

Table I

Electrical Power Stored Across The Stationary Joints During AC Current Flow, Prior and Following Exposure To The So_2.

Material Type	Reference Sample	After SO_2 Exposure
silver contacts on brass substrate	19.28 ± 0.4 W	18.70 ± 0.6 W
silver contacts on copper substrate and silver plated	8.51 ± 0.2 W	9.02 ± 0.4 W

B. Surface Investigation by Scanning Electron Microscopy (SEM) and by Energy Dispersive Analysis (EDS)

B.1. Plain silver contacts – This section provides SEM microphotos and EDS analysis results of silver contacts welded on top of brass alloy (70% Cu 30% Zn), or copper substrates. The copper substrate contacts were also silver plated. It investigates the corrosion induced degradation as a result of SO_2 exposure, and electrical erosion produced during the current cycling tests.

B.1.a. The pristine condition: Figure 10 shows the surface condition of the Ag contact in its pristine state, i.e. before exposure in the aggressive environment, as seen by SEM. The surface under high magnification is not smooth but has certain irregularities, which may act as nucleating sites, and corrosion initiation centers where water collects as pools and drops.

B.1.b. Following the SO_2 exposure: In Figures 11(a),(b) and (c), the Ag electrical contact welded on top of the silver plated copper substrate, is shown after an exposure of 24h in a SO_2-air environment. The Ag contact

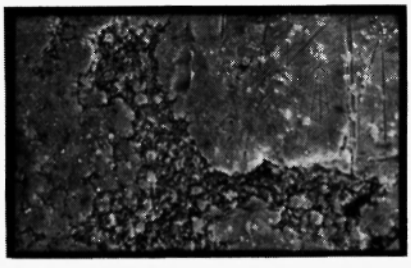

Fig. 10: (x1600) Typical SEM micrograph of the virgin Ag electrical contact surface.

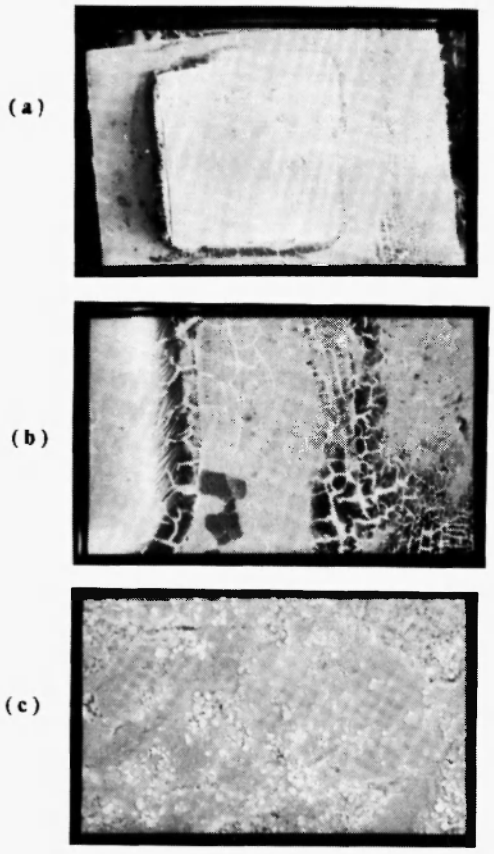

Fig. 11: **(a)** (x 22) Ag contact on copper substrate/silver plated after 24 h exposure in SO_2-air environment. Cracks are formed on the silver plating. The welding material at the periphery of the silver contact has been separately attacked. **(b)** (x 80) Detail in the welding region between the contact and the substrate. Cracks are formed on the welding layers by the corrosion compounds. **(c)** (x 1600) The surface of the electrical contact is covered by small crystals.

region is in very good condition as opposed to the suspending brass substrate, which is heavily attacked and there is an extensive production of deep cracks along the corrosion surface compounds. These are found to be mainly copper sulfates. The welding zone is also separately attacked with distinct formation of corrosion products near the heat-affected zone. The surface of the contact

region is covered by the scattered small particles that have a composition by EDS of Ag: 38%, Cu: 60% and Zn: 1.5%. Their originating mechanism cannot be singularly identified and requires further investigation.

Figures 12(a) and (b), provide micrographs of an Ag contact on top of a brass wafer after exposure to SO_2-air with equilibrium humidity. The overall electrical contact material seems to be totally unaffected by such exposure. The brass wafer is completely attacked, even visually, as there are formed thick layers of green-blue deposits, mainly corrosion products of the brass alloy such as copper-zinc hydrated sulfates.

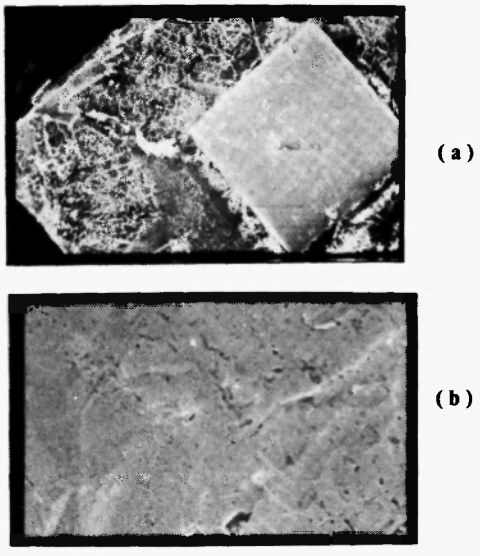

Fig. 12: **(a)** (x22) Ag contact on brass wafer after 24 h in SO_2-air environment. The Ag surface appears unaffected as opposed to the brass, which is covered by voluminous corrosion products. **(b)** (x1600) Close-up of the Ag contact region. The surface, even under high magnification seems unaffected.

B.1.c. Following the electrical fatigue: In the following micrographs, the same electrical contact joints are examined by SEM and EDS analysis after their current switching cycle tests.

Figures 13(a) and (b), show the reference contact joint (i.e. not exposed to the adverse environment) of Ag on brass substrate after being subjected to switching current cycle tests. A crater is formed on the anodic Ag surface, by

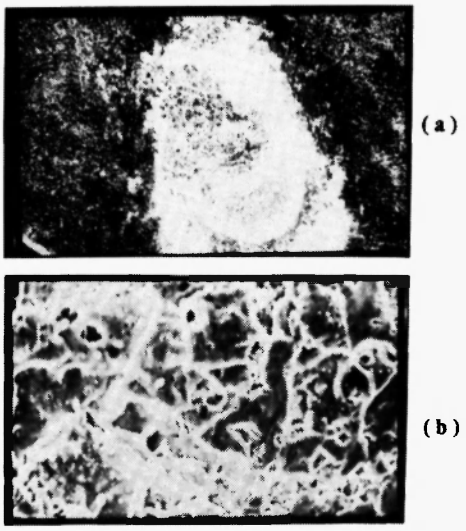

Fig. 13: **(a)** (x100) Ag contact on brass substrate after current cycling test. The shortest diameter of the oval crater formed on the contact is approximately 400μm. The material on the rims of the crater is remelted and resolidified and the crystal edges are rounded. **(b)** (x1600) the bottom layer of the crater with resolidified Ag crystals.

the plasma formation during arcing, resulting to mass and energy transfer between the joints.

Figures 14(a) and (b), show the Ag contact on silver plated copper substrate after 24h exposure in a SO_2-air environment and after current switching cycle tests. The surface of the silver contact has a crater with a very deep pit on one side. The pit depth was measured by optical microscopy to be around 190μm. The material at the crater is remelted by the heat produced by plasma formation during arcing and this is shown in the higher magnification scale of the surface.

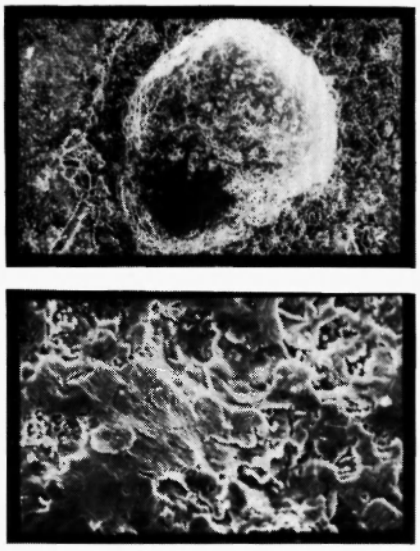

Fig. 14: **(a)** Ag on silver plated copper substrate after an exposure of 24h in a SO_2-air environment and after current switching cycle tests, (x 160) the crater on the contact with one side pit.. **(b)** (x 600) The resolidified material of the shallow side of the crater.

In Figures 15(a),(b), and (c), the Ag on brass wafer is shown after 24h exposure in a SO_2-air environment and after the current switching cycle tests. The crater in not very deep but the surface of the wafer was found to be seriously affected by the formation of sulfate crystals. The welding area is also heavily attacked by the adverse environment. The EDS analysis gave the following composition of products on the welding material: S:36%, Zn:43%, Ni: 6.69%, Cu: 13.6%.

B.2. Ag/CdO electrical contacts: This section provides SEM microphotos of the Ag/CdO electrical contacts welded on top of brass (Cu 70%, Zn 30%) substrates. The effect of plating is investigated.

B.2.a. Unplated joints: In Fig. 16(a), the Ag/CdO contact on brass substrate after exposure in the SO_2 chamber with equilibrium humidity is shown after sustaining 20,000 current switching cycles test. Most of the Ag/CdO surface (≅30%) suffered melting and resolidification and the whole electrical contact area is covered by silver spherules produced by resolidification [Fig.16(b)]. No crater formation is encountered. Most of the

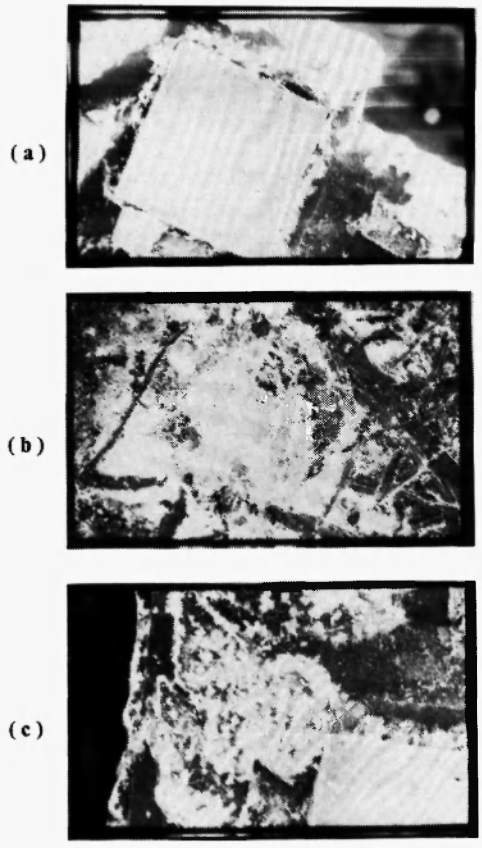

Fig. 15: **(a)** (x 22) Ag on top of brass substrate, shown after the exposure of 24h in a SO_2-air environment and after the current switching cycle tests. **(b)** (x 100) Crater formed on the surface of the contact with a 300μm diameter. **(c)** (x 35) The welding zone bed, with crystals formed on the wafer.

corrosion products are accumulated aside the welding area at the base of the contact.

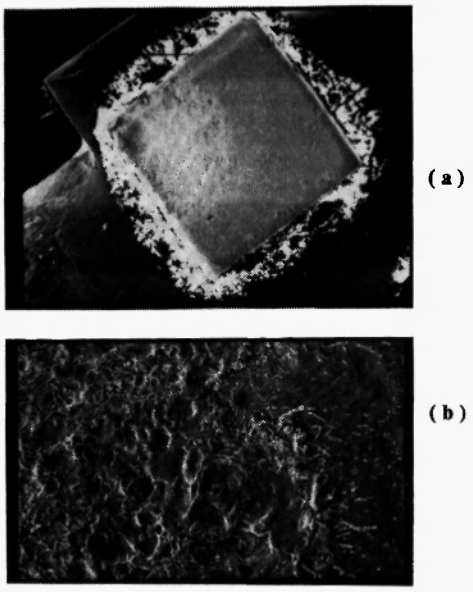

Fig. 16: **(a)** (x 25), Ag/CdO contact on brass substrate after exposure in the SO_2 chamber. A contact after sustaining the 20,000 current switching cycles test. **(b)** (x 100). Resolidification of the melted silver/ cadmium oxide contact material.

B.2.b. Silver plated joints: In Fig. 17(a) the Ag/CdO contact welded on brass substrate and then silver plated is shown after exposure in the SO_2 chamber. Many crystals are set on the surface of the contact material. In Fig. 17 (b) one loosely attached crystal of the corrosion products, consisting mainly of hydrated copper and zinc sulfates is presented. It lies on the surface of the contact material and it does not adhere on the silver plating. The surface of the contact is relatively smooth. During the current cycle tests, all of these deposits fall off, due to the mechanical vibration and low adhesion. In Fig. 17 (c) the contact surface is presented after sustaining a 20,000 cycles current switching test. The eroded surface covers approximately 45% of the contact material and is more extended compared to the erosion patterns observed on the unplated brass samples.

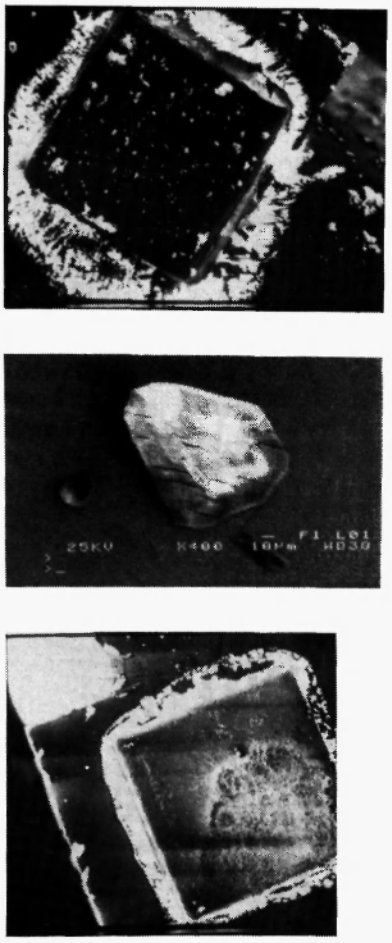

Fig. 17: **(a)** (x 25) Ag/CdO contact welded on brass substrate and then silver plated, after being exposed in the SO_2 environment. **(b)** (x 400) Corrosion products of hydrated copper and zinc sulfates. **(c)** (x 25) The surface after sustaining 20,000 current switching cycles.

B.2.c. Gold plated joints: In Fig. 18(a) the Ag/CdO contact on brass substrate and gold plated is presented after exposure in the SO_2 environment. On the surface there is a formation of corrosion products, at specific nucleating sites, originating from the sides of the welding areas. A dark formation was zoomed in and a linear series of cracks is observed in Fig.

18(b). A lift off of the gold overlayer is initiated where the crystallization of the crept corrosion product occurs. In Fig. 18(c) a dendrite type formation begins its expansion on the surface by cracking the gold plating.

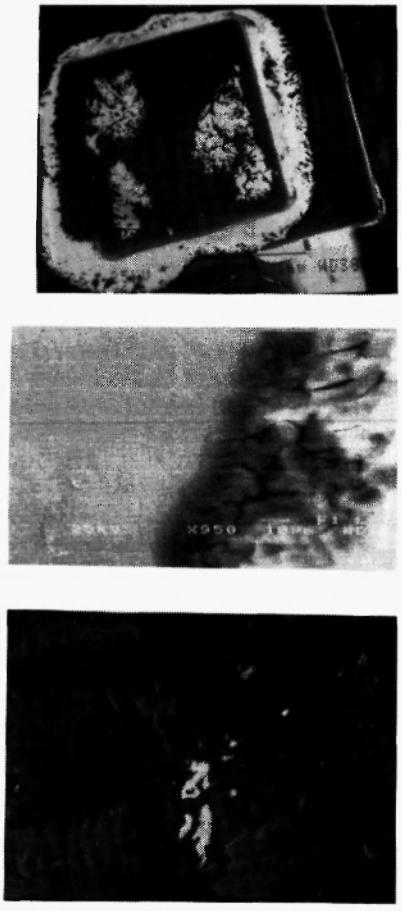

Fig. 18: (a) (x 25) Ag/CdO contact welded on a brass substrate and then gold plated, after exposure in the SO_2 environment. **(b)** (x 950) Linear series of cracks. **(c)** (x 400) A dendrite type formation by cracking off the gold plating.

Figs. 19 (a), (b) demonstrate the effect of the number of the current switching cycles on the extent of erosion over the contact, material (gold plated Ag/CdO). As expected, the damaged area is more expanded at the

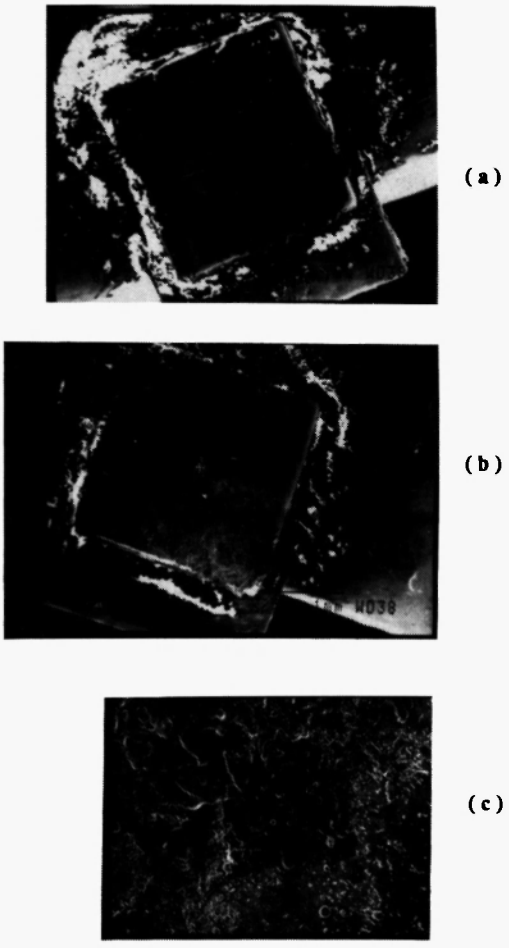

Fig. 19: (a),(b) (x 25): Erosion of the surface of the gold plated contact **(a)**: 6,000 cycles, **(b)** 20,000 cycles. **(c)** (x 1500) Extended porosity encountered on the eroded contact.

20,000 cycles than the 6,000 cycles. The eroded area also exhibits a significant number of pores after the resolidification of the surface material as seen in Fig. 19(c) under high magnification.

Some general remarks drawn from weight change measurements of the examined contact materials before, and following their exposure to the SO_2, as well as after their electrical fatigue, may be summarized as follows:

- The pure silver contact materials tend to produce well shaped hillocks or

craters (depending on polarity) after their current cycle tests.

- The Ag/CdO contacts end-up with extended melting resolidification of the surface material and reduced material migration effects.
- The SO_2 exposure of the joints increases their net weight by 2% as a result of corrosion layer or byproduct formations.
- Most of corrosion products are soluble in water (≈1.8% joint weight), while others are loosely attached.

C. Interpretation Of Contact Degradation Mechanisms

During the current cycle tests of the plain silver electrical contacts, the material transfer occurred from the stationary anode towards the cathode electrode, thus forming localized hillocks on the cathode and deep craters on the anode. The crater is formed on the surface after current switching cycle tests and has smaller dimensions for the silver plated copper substrate samples compared to the un-plated brass substrate samples. This could be explained by the more efficient heat dissipation rates offered by the silver plated copper substrates, leading to lower interfacial temperature transition zones. The typical mass transfer for the brass substrate samples was weighted to be 25mg on a total average sample weight of 0.8000g. On the Ag/CdO contacts, under exactly the same electrical fatigue testing procedure, there was not a crater or hillock formed but an extended surface area was eroded with silver melting and resolidifying. Also the weight change due to the mass transfer was very insignificant, of the order of 5 mg or less (close to the measurement sensitivity). This was also systematic for all types of plating. SO_2 exposure increased the extent of eroded surface, compared to the non-exposed specimens.

The electrical contacts may have different erosion characteristics as a result of switching operations and load types[22]. Material transfer from anode to cathode is always observed in contact make-only switching. In the break-only switching the material transfers during *short arcs* is from anode to cathode, while in the *long arcs* (usual case) is from cathode to anode[23]. In the normal operating contact mode (make and break) net material transfer is determined by the combined action of make-transfer (anode to cathode) and break-transfer (cathode to anode)[24]. Contact bounce is undesirable and causes make-operation contact erosion. In that case, the dynamic welding results in low contact resistance, and the material transfer is from anode to cathode forming localized hillocks and craters. McBride examined contact bounce in

relays and has found material transfer to be both, current dependent and surface morphology sensitive[25]. Therefore, generalized approaches concerning material transfer during current cycling will have to consider the long arc, short arc, and asymmetry bridge theories, in order to describe the observed mass transfer phenomena [22].

The surface analysis during the different stages of the testing sequence shows that the corrosion byproducts on the contact proper are characterized by low adhesion properties. Upon current cycling tests all loose deposits are removed (except from the vertical walls of the welding layers aside the contact region) either by the electrostatic effects induced by arcing or by the mechanical vibrations produced during the movement of the contact joints.

For the investigated structures of the contact joints the exposure in the SO_2 induces corrosion products. The corrosion layers on top of the brass substrates have to be cleared mechanically in order to enable for electrical conduction at the clamping edge of the substrate. The edges of the welding layers that extend beyond the contact material are heavily attacked by the SO_2 environment. The Cu, and Ni ions (of the welding material) diffuse through the pores of the silver plating during the exposure in an active electrolyte i.e. aqueous solution with SO_4^{2-} and form corrosion products on the surface of the wafer which can be transported to the general surface. The presence of salt concentrations cells assists corrosion reactions [26].

According to the electrical performance of the plated Ag/CdO specimens, the ones with the silver plated brass substrate exhibit higher durability to SO_2 exposures compared to gold plated brass substrates. This is also confirmed by SEM observations. The plating should have the minimum of defects and pores, otherwise the substrate ions would diffuse to form corrosion products especially when assisted by the presence of strong electrolytes. In general, the smaller the initial size of the pore, the smaller the eventual corrosion site and the cleaner the surface even after long term exposure to severely corrosive environment.

There is a galvanic cell formation between the silver and the brass wafer. This effectively protects the silver end of the cell and increases the corrosion effects on the less noble material, which is brass.

IV. CONCLUSIONS.

The physical properties of the suspending wafers of the electrical contacts should be carefully considered by component designers in order to allow for maximum heat dissipation during device operation, as well as, to minimize corrosion product formations when operating in adverse environments. For example, plain silver contacts welded on top of copper substrates, and then silver plated, offer higher nominal currents compared to identical contacts welded on top of brass substrates. This has been experimentally confirmed by dc temperature overheat tests, as well as by measurements of the electrical energy storage during ac operation.

Contacts may exhibit vastly different behavior when operated under adverse environmental conditions depending on material synergy effects. The long-term operation and response of the electrical contacts in a corrosive environment strongly depends upon the corrosion rate and the electrochemical reaction kinetics.

Brass substrates corrode rather heavily when exposed to SO_2 environment, forming insulating copper-zinc sulfate thick films. However, the presence of the brass surface aids the good performance of the silver contact by acting as a sacrificial anode. This fact could be practically exploited by the manufacturers by allowing a part of the surface to act sacrificially when the conditions of operation preclude the presence of a very aggressive working environment. Thus, the contact would remain mostly unaffected and the brass would corrode.

The electroplating material, pore size, and the plating anomalies, are very important parameters in determining the diffused corrosion product size and/or concentration over the contact proper.

REFERENCES

1. R. Holm, *Electric Contacts*, Springer Verlag, Berlin, 1967.
2. P.G. Slade, Y.K. Chien and J.A. Bindas, *IEEE Trans. Comp., Hybrids, Manufact. Technol.*, 13, No. 1, 2 (1990).
3. T.E. Graedel, , *J. Electrochem. Soc.*, Vol. 139, No. 7, 1963 (1992).
4. P.G. Slade, *IEEE Trans. Comp., Hybrids, Manufact. Technol*, 9, No. 1, 3 (1986).
5. W.H. Abbott, "The development and performance characteristics of

mixed flowing gas test environments", in *Proc. 33rd IEEE Holm Conf. on Electrical Contacts*, p.63, (1987).

6. R. Geckle and R.S. Mroczkowski, *IEEE Trans. Comp., Hybrids, Manufact. Technol.*, 14, No. 1, 162 (1991).
7. W.H. Abbott, *Rev. Gen. Electricite*, 16, 58 (1989).
8. M. Antler, *IEEE Trans. Comp., Hybrids, Manufact. Technol., CHMT-5*, 301 (1982).
9. R.W. Chiarenzelli, and E.L. Joba, *J.Air Pollut. Contr. Assoc.*, 16, 123 (1966).
10. W.H. Abbott, *IEEE Trans. Parts, Hybrids, Packaging*, PHP-10, 24 (1974).
11. W.H. Abbott, "*Electrical Contacts/1970*", Chicago IIT Research Institute, pp.21-25, (1970).
12. ASTM Designation: B827- 92 "*Standard Practice for Conducting Mixed Flowing Gas (MFG) Environmental Tests*" (1992).
13. ASTM Designation: B 845 - 93, "*Standard Guide for Mixed Flowing Gas (MFG) Tests for Electrical Contacts*", (1993).
14. I.L. Rozenfeld, "*Atmospheric Corrosion of Metals*", National Association of Corrosion Engineers, Houston, (1972).
15. R.B.Comizzoli, J.P. Franey, T.E. Graedel, G.W. Kammlott, A.E.Miller, A.J. Muller, G.A. Peins, L.A. Psota-Kelty, J.D.Sinclair, R.C. Wetzel, *J.Electrochemical Society*, 139, 2058 (1992).
16. M. Ausloos, *Bull. Sci. Assoc. Ing. Electr. Inst. Electrotech. Montefiore (Belgium)*, 102, No. 2, 22 (1989) *in French.*
17. D.C. Arney and B.T. Robinson, *Comput. Math. Appl.*, 19, No.3, 1 (1990).
18. C.T. Dervos and J. Michaelides, "The effect of contact capacitance on current-voltage characteristics of stationary metal contacts", in *Proc. of 43rd IEEE Holm Conf. on Electrical Contacts*, pp.152-164, Philadelphia PA, (1997).
19. C.T. Dervos and P.T. Fitsilis, *IEEE Trans. Comp. Packaging, Manuf. Technol. -Part A.*, 17, No. 2, 286 (1994).
20. C.T. Dervos, C.G. Karagiannopoulos, P.D. Bourkas, and C.A. Kagarakis, *IEE Proc. Pt.C*, 140, No. 3, 167 (1993).
21. C.T. Dervos, "Implications of positive ion layer formation across highly injecting metal contacts: Current instabilities and electrostatic repulsion", in *Proc. of 41st IEEE Holm Conf. on Electrical Contacts*, pp. 175-185, Montreal, (1995).

22. C.H. Leung and A. Lee, "Contact erosion in automotive dc relays", in *Proc. of 36th Holm Conf. on Electrical Contacts*, pp. 85-93, (1990).
23. F. Llwellyn-Jones, "Erosion Processes and assessment of electrical contact materials", in *Proc. 24th Holm Conf. on Electrical Contacts*, pp. 249-254, (1978).
24. M. Sato, *Trans. Nat. Res. Inst. of Metals*, 18, No. 2, 65 (1976).
25. J.W. McBride, *IEEE Trans. Comp., Hybrids, Manufact. Technol.*, 12, No. 1, 82 (1989).
26. Y. Fukushima, K Fukuda,., Kurosawa, S., Judabong, P.C. Sabularse, "Environmental Factors Affecting Corrosion and Discoloration of Metals in the Indoor Atmosphere", *Proc. on Corrosion Effects of Acid Deposition and Corrosion of Electronic Materials*, Eds. F. Mansfeld, V. Kucera, S. Haagenrud, F.H.Haynie, J.D.Sinclair, The Electrochemical Soc.,Vol.86-6, pp.338-346, (1986).